

Design of Neural Network and Backstepping based Adaptive Flight Controller for Multi-Effector UAV

Liwei Qiu, Guoliang Fan, Jianqiang Yi, and Wensheng Yu

Abstract—Research of modern flight control methods for unmanned aerial vehicles (UAVs), which lower the cost and risk associated with the design of actual physical flight systems, has become research hotspot in recent years. However, design of control laws for UAV is complicated and challengeable due to UAV uncertainties, nonlinearity and coupling. This paper proposes a new hybrid controller design scheme, which consists of a backstepping controller and a neural network compensator. The backstepping controller realizes linearization and decoupling of the highly nonlinear and tightly coupled UAV model. For cancelling out uncertainties such as unmodeled dynamics and external disturbances, the neural network compensator is designed to enhance the robustness of flight system. Pseudoinverse method is applied to establish the mapping between moments and multiple control surfaces. Numerical simulation shows that the UAV equipped the hybrid controller has good maneuverability, strong self-learning ability of compensating the unmodeled dynamics and enough robust stability against constraints of actuators.

I. INTRODUCTION

Design of flight control methods for UAVs is crucial technology in aviation industry all the time. As early as 1899, Wilber Wright started considering one of three basic flight questions, that was, how to control “Flyer” in the air. The Brothers invented the classical three-axis control system, which realized roll, pitch and yaw by selecting appropriate deflection angles of aileron, elevator and rudder respectively. With the advent of high performance aircraft, traditional design scheme of gain-scheduling is far from meeting the requirement for promoting flight performance[1]. In order to bring benefits of lowering the cost and risk associated with the design of actual physical flight systems, it is hoped that modern flight control scheme should be established.

Modern UAV dynamics is multi-input-multi-output, tightly coupled and highly nonlinear. In most engineering applications, it is always common to adopt gain scheduling scheme. Gain scheduling is an approach to design a family of linear controllers, each of which provides satisfactory flight quality for different operating domain of the whole flight envelope. The scheduling variables(eg:Mach number or flight height) are used to determine appropriate linear controller. However,

This work was supported by CAS Innovation Projects (Grant Nos. CXJJ-09-M27 and ZKYG09A02) and the National Natural Science Foundation of China (Grant Nos. 60874010, 60621001).

L. Qiu, G. Fan, J. Yi, and W. Yu are with Institute of Automation, Chinese Academy of Sciences, Beijing, P.R.China liwei.qiu@ia.ac.cn, glfan@hitic.ia.ac.cn, jianqiang.yi@ia.ac.cn, wsyu@sei.ecnu.edu.cn

W. S. Yu is also with Shanghai Key Laboratory of Trustworthy Computing, East China Normal University, Shanghai, P.R.China

the switch of different linear controllers isn't always smooth. It is urgent that a single controller designed could run well for a certain flight envelope.

In order to solve such a tough question encountered in using gain scheduling scheme for a certain flight envelope, numerous flight control algorithms, such as linear quadratic gaussian[2], eigenstructure assignment[3], H_2/H_∞ mixed control [4], feedback linearization [5], backstepping[6,7] etc have emerged, most of which have been verified successfully in linear or nonlinear aircraft models. Among such methods, feedback linearization and backstepping are the most prominent in that they successfully solved the puzzle of decoupling and linearization of flight vehicle dynamics[8]. Using feedback linearization, as the name implies, the nonlinear and coupled aircraft dynamics is replaced by the linear model through the wonders of feedback. Backstepping is a technique based on Lyapunov theory developed in 1990s by P. V. Kokotovic and others[8], which is applicable for a special class of nonlinear lower triangular structure dynamical systems. Because of this recursive structure, design process starts from the known-stable system and backs out new controllers that progressively stabilize each outer subsystem. The process terminates when the final external control is reached. However, the two control schemes mentioned above severely rely on exact model of flight vehicles known in advance. This assumption is not always realistic in practical flight control systems due to unmodeled dynamics, sensor measuring noise, wind gusts, etc. How to eliminate effects of the uncertainties is important for achieving good handling qualities and strong robustness. Several results combining feedback linearization, backstepping with robust control methods have been achieved. Ngo, Reigelsperger and Banda linked feedback linearization with structured singular value synthesis in tailless aircraft control [9]. Johnson, Calise and Corban adopted a neural network approach to compensate the uncertainties in the design of X-33 [10]. Sonneveldt, Chu and Mulder applied constrained adaptive backstepping to a nonlinear F-16 MATV model[11,12].

In this paper, in order to overcome difficulties stemming from unmodeled dynamics, sensor measuring noise, wind gusts, we present a new hybrid control scheme to analyze and design flight control systems. The paper is organized as follows: Section II is devoted to describing the UAV model. In Section III, the framework of the hybrid control scheme is proposed and detailed design procedure of the controller is given. Section IV explains the numerical simulation results that show the robust performance. Conclusions are drawn in Section V.

II. UAV DYNAMIC MODEL DESCRIPTION

It is more convenient to express motion of UAV in the body-axis reference frame compared to wind-axis reference frame. Fig. 1 describes the analysis of aerodynamic force and moment in the body-axis reference frame[13]. In the body-axis reference frame, the origin O_U is at the UAV centre of gravity. C_l, C_m, C_n are aerodynamic moment coefficients along the X_U, Y_U, Z_U axes respectively, C_T, C_C, C_N are aerodynamic force coefficients along the X_U, Y_U, Z_U axes respectively.

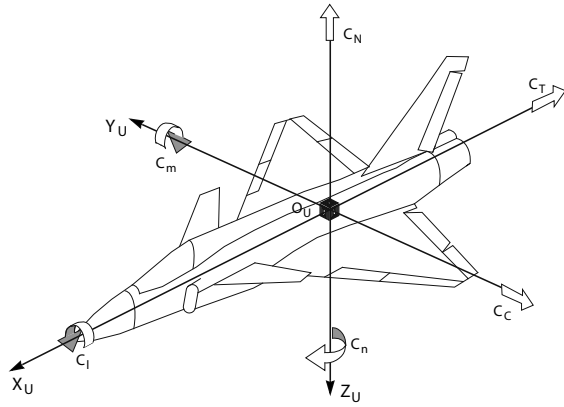


Fig. 1. Analysis of aerodynamic force and moment in the body-axis reference frame

Assumption 1 : The UAV is a rigid-body, which means that any two points on or within the airframe remain fixed with respect to each other.

Assumption 2: The mass distribution of the UAV is symmetric relative to $X_U O_U Z_U$ plane, this implies that the products of inertia I_{yz} and I_{xy} are equal to zero.

Based on Assumption 1 and Assumption 2, moment dynamics equations of the mass centre in the body-axis reference frame are described as follows [14].

$$\begin{aligned}\dot{\phi} &= p + \tan \theta (q \sin \phi + r \cos \phi) \\ \dot{\theta} &= q \cos \phi - r \sin \phi \\ \dot{\psi} &= \frac{q \sin \phi + r \cos \phi}{\cos \theta} \\ \dot{p} &= (c_1 r + c_2 p) q + c_3 L + c_4 N \\ \dot{q} &= c_5 p r - c_6 (p^2 - r^2) + c_7 M \\ \dot{r} &= (c_8 p - c_2 r) q + c_4 L + c_9 N\end{aligned}\quad (1)$$

$$\begin{aligned}C_C &= C_{c_0}(\alpha, \beta) + \delta C_{c_{\delta_a}}\left(\frac{\delta_a}{21.5}\right) + \delta C_{c_{\delta_r}}\left(\frac{\delta_r}{30}\right) \\ &\quad + \frac{rb}{2V_T} C_{c_r}(\alpha) + \frac{pb}{2V_T} C_{c_p}(\alpha) \\ C_N &= C_{N_0}(\alpha, \beta, \delta_e) + \frac{q\bar{c}}{2V_T} C_{N_q}(\alpha) \\ C_l &= C_{l_0}(\alpha, \beta, \delta_e) + \delta C_{l_{\delta_a}}\left(\frac{\delta_a}{21.5}\right) + \delta C_{l_{\delta_r}}\left(\frac{\delta_r}{30}\right) \\ &\quad + \frac{rb}{2V_T} C_{l_r}(\alpha) + \frac{pb}{2V_T} C_{l_p}(\alpha) + \delta C_{l_\beta} \beta \\ C_m &= C_{m_0}(\alpha, \beta, \delta_e) + C_N(x_{cgr} - x_{cg}) + \frac{q\bar{c}}{2V_T} C_{m_q}(\alpha)\end{aligned}\quad (2)$$

$$\begin{aligned}C_n &= C_{n_0}(\alpha, \beta, \delta_e) + \delta C_{n_{\delta_a}}\left(\frac{\delta_a}{21.5}\right) + \delta C_{n_{\delta_r}}\left(\frac{\delta_r}{30}\right) \\ &\quad + \frac{rb}{2V_T} C_{n_r}(\alpha) + \frac{pb}{2V_T} C_{n_p}(\alpha) + \delta C_{n_\beta}(\alpha) \beta \\ &\quad - C_C(x_{cgr} - x_{cg}) \frac{\bar{c}}{b} \\ L &= C_l \cdot Q \cdot S \cdot b + T(-\delta_x y_T - \delta_y z_T) \\ M &= C_m \cdot Q \cdot S \cdot \bar{c} + T(\delta_z x_T + z_T) \\ N &= C_n \cdot Q \cdot S \cdot b + T \delta_y x_T\end{aligned}\quad (3)$$

where ϕ, θ, ψ are roll, pitch, yaw angles, p, q, r are body-fixed roll, pitch, yaw rates, α, β are angle of attack and angle of sideslip, L, M, N are moments along the X_U, Y_U, Z_U axes respectively, $\delta_e, \delta_a, \delta_r$ are deflections of elevator, aileron, rudder, T is thrust force, x_T, y_T, z_T are coordinates of installation location of the engine in the body-axis reference frame, $\delta_x, \delta_y, \delta_z$ are deflections of thrust vector, Q, S, b, \bar{c} are dynamic pressure, wing area, wing span and mean aerodynamic chord, $c_1 = \frac{(I_y - I_z)I_z - I_{xz}^2}{\Sigma}, c_2 = \frac{(I_x - I_y + I_z)I_{xz}}{\Sigma}, c_3 = \frac{I_z}{\Sigma}, c_4 = \frac{I_{xz}}{\Sigma}, c_5 = \frac{I_z - I_x}{I_y}, c_6 = \frac{I_{xz}}{I_y}, c_7 = \frac{1}{I_y}, c_8 = \frac{I_x(I_x - I_y) + I_{xz}^2}{\Sigma}, c_9 = \frac{I_x}{\Sigma}, \Sigma = I_x I_z - I_{xz}^2, I_x, I_y, I_z, I_{xz}$ are $x, y, z, x-z$ body moments of inertia. $C_{c_0}, \delta C_{c_{\delta_a}}, \dots, \delta C_{n_\beta}$ are nondimensional aerodynamic coefficients, which are obtained from wind tunnel experiments and have been stored in lookup tables as a function of current flight condition.

III. ROBUST HYBRID CONTROL SCHEME DESIGN

In order to track attitude angles more effectively, an adaptive hybrid control scheme is proposed in this section. As is depicted in the Fig. 2, the robust hybrid control scheme proposed consists of a backstepping controller and a neural network compensator so as to guarantee stability and robustness of the UAV dynamics. The role of the backstepping controller is to ensure the stability of nominal UAV dynamics throughout the flight envelope via twice “step back”. Considering the unmodeled dynamics and external disturbance, a neural network compensator using RBFNN is adopted to ensure robust stability and performance of flight system, which is realized via the appropriate adaptive compensation. Control law allocation is introduced in order to establish the mapping relationship between moment and multiple control surface.

A. Design of the Backstepping Controller

UAV dynamics can be represented into the following compact form so as to adopt backstepping method conveniently. Equation (1) is expressed as follows.

$$\begin{aligned}\dot{x}_1 &= \begin{bmatrix} \dot{\phi} \\ \dot{\theta} \\ \dot{\psi} \end{bmatrix} = \begin{bmatrix} p + \tan \theta (q \sin \phi + r \cos \phi) \\ q \cos \phi - r \sin \phi \\ \frac{q \sin \phi + r \cos \phi}{\cos \theta} \end{bmatrix} \\ &= \begin{bmatrix} 1 & \tan \theta \sin \phi & \tan \theta \cos \phi \\ 0 & \cos \phi & -\sin \phi \\ 0 & \frac{\sin \phi}{\cos \theta} & \frac{\cos \phi}{\cos \theta} \end{bmatrix} \begin{bmatrix} p \\ q \\ r \end{bmatrix} \\ &= f_{11}(x_1) \cdot x_2\end{aligned}\quad (4)$$

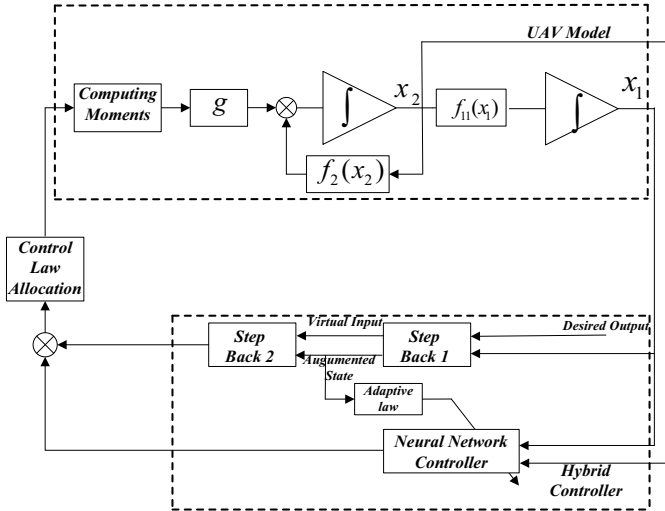


Fig. 2. Block diagram of the robust hybrid control system

$$\text{where } x_1 = \begin{bmatrix} \phi \\ \theta \\ \psi \end{bmatrix}, x_2 = \begin{bmatrix} p \\ q \\ r \end{bmatrix}.$$

Time derivative of $f_{11}(x_1)$ is obtained as follows.

$$\dot{f}_{11}(x_1) = \begin{bmatrix} 0 & (\tan \theta \sin \phi)' & (\tan \theta \cos \phi)' \\ 0 & (\cos \phi)' & (-\sin \phi)' \\ 0 & (\frac{\sin \phi}{\cos \theta})' & (\frac{\cos \phi}{\cos \theta})' \end{bmatrix}$$

where

$$\begin{aligned} (\tan \theta \sin \phi)' &= \sec^2 \theta \sin \phi (q \cos \phi - r \sin \phi) + \\ &\quad \tan \theta \cos \phi (p + \tan \theta (q \sin \phi + r \cos \phi)) \\ (\tan \theta \cos \phi)' &= \sec^2 \theta \cos \phi (q \cos \phi - r \sin \phi) - \\ &\quad \tan \theta \sin \phi (p + \tan \theta (q \sin \phi + r \cos \phi)) \\ (\cos \phi)' &= -\sin \phi (p + \tan \theta (q \sin \phi + r \cos \phi)) \\ (-\sin \phi)' &= -\cos \phi (p + \tan \theta (q \sin \phi + r \cos \phi)) \\ (\frac{\sin \phi}{\cos \theta})' &= [\cos \phi \cos \theta (p + \tan \theta (q \sin \phi + r \cos \phi)) \\ &\quad + \sin \phi \sin \theta (q \cos \phi - r \sin \phi)] / (\cos^2 \theta) \\ (\frac{\cos \phi}{\cos \theta})' &= [-\sin \phi \cos \theta (p + \tan \theta (q \sin \phi + r \cos \phi)) \\ &\quad + \cos \phi \sin \theta (q \cos \phi - r \sin \phi)] / (\cos^2 \theta) \end{aligned}$$

Equation (2) is expressed as follows in a similar way.

$$\begin{aligned} \dot{x}_2 &= \begin{bmatrix} \dot{p} \\ \dot{q} \\ \dot{r} \end{bmatrix} = \begin{bmatrix} (c_1 r + c_2 p) q \\ c_5 p r - c_6 (p^2 - r^2) \\ (c_8 p - c_2 r) q \end{bmatrix} \\ &+ \begin{bmatrix} c_3 & 0 & c_4 \\ 0 & c_7 & 0 \\ c_4 & 0 & c_9 \end{bmatrix} \begin{bmatrix} L \\ M \\ N \end{bmatrix} \\ &= f_2(x_2) + g \cdot u \\ &= g^* \cdot u + \Delta \end{aligned} \quad (5)$$

Because measuring error of moment of inertia I_x, I_y, I_z, I_{xz} always exists, exact values of $c_i (i = 1 \sim 9)$

are difficult to obtain, which means that $f_2(x_2), g$ is partly known in advance. Nominal value of $f_2(x_2), g$ is denoted as $f_2^*(x_2), g^*$, and $f_2(x)$ fluctuates more widely compared with g considering that $f_2(x)$ is also a function of roll, pitch and yaw rate. That's to say, g^* is relatively reliable, therefore, the uncertainty Δ is represented as $f_2(x) + [g - g^*]u$. Since neural network has an ability of approximating a nonlinear continuous function to arbitrary accuracy, a RBFNN is adopted to approximate Δ .

$$\Delta = W \cdot \phi(\xi) + \varepsilon$$

where W is the weighting matrix of RBFNN,

$$W = \begin{bmatrix} w_{11} & \cdots & w_{1,\text{node}} \\ w_{21} & \cdots & w_{2,\text{node}} \\ w_{31} & \cdots & w_{3,\text{node}} \end{bmatrix}, \xi = \begin{bmatrix} \phi \\ \theta \\ \psi \\ p \\ q \\ r \end{bmatrix}$$

$\phi(\xi) = e^{-\frac{\|\xi - c\|^2}{2\sigma^2}}$ is the excitation function vector, c is the centre vector of the excitation function, σ is the width of the excitation function, ε is an arbitrarily small constant vector, node is the node number of hidden layer.

The optimal parameter matrix W^* defined is a quantity only for analytical purpose. Typically W^* is chosen as the value of W that minimizes $f_2(x) + [g - g^*]u$

That's,

$$W^* = \arg \min_{W \in R^n} \{ \sup_{x \in \Omega} \{ f_2(x) + [g - g^*]u \} \}$$

W^* varies slowly and is bounded, that is, $\|W^*\|_F \leq \varrho$, where ϱ is a positive real number, $\|\cdot\|_F$ denotes Frobenius norm.

Supposing $q_{ref}(t)$ is the desired output of UAV dynamics, the error between x_1 and its desired value is defined as

$$z_1 = x_1 - q_{ref}(t)$$

therefore, $\dot{z}_1 = \dot{x}_1 - \dot{q}_{ref}(t) = f_{11}(x_1) \cdot x_2 - \dot{q}_{ref}(t)$

Constructing the following Lyapunov function

$$V_1 = \frac{1}{2} z_1^T \cdot z_1,$$

we obtain that

$$\begin{aligned} \dot{V}_1 &= z_1^T \cdot \dot{z}_1 \\ &= z_1^T \cdot [f_{11}(x_1) \cdot x_2 - \dot{q}_{ref}(t)] \\ &= z_1^T \cdot [f_{11}(x_1) \cdot x_2 - \dot{q}_{ref}(t) - a_1(t) + a_1(t)] \end{aligned}$$

Given virtual input $a_1(t) = -C_1 \cdot z_1 (C_1 > 0)$ and augmented state $z_2 = f_{11}(x_1) \cdot x_2 - \dot{q}_{ref}(t) - a_1(t)$, it's straightforward to obtain

$$\dot{V}_1 = -C_1 \cdot \|z_1\|^2 + z_1^T \cdot z_2$$

If $z_2 \rightarrow 0$, then $\dot{V}_1 < 0$, $z_1 \rightarrow 0$. We easily obtain

$$\dot{a}_1(t) = -C_1 \cdot \dot{z}_1 = -C_1 \cdot [f_{11}(x_1) \cdot x_2 - \dot{q}_{ref}(t)]$$

$$\begin{aligned}\dot{z}_2 &= \dot{f}_{11}(x_1) \cdot x_2 + f_{11}(x_1) \cdot \dot{x}_2 - \ddot{q}_{ref}(t) - \dot{a}_1(t) \\ &= \dot{f}_{11}(x_1) \cdot x_2 - \ddot{q}_{ref}(t) - \dot{a}_1(t) + f_{11}(x_1) \cdot g^* \cdot u + f_{11}(x_1) \cdot (W \cdot \phi + \varepsilon)\end{aligned}\quad (6)$$

Constructing the second Lyapunov function

$$V_2 = V_1 + \frac{1}{2} z_2^T \cdot z_2$$

$$\begin{aligned}\dot{V}_2 &= -C_1 \cdot \|z_1\|^2 + z_1^T \cdot z_2 + z_2^T \cdot \dot{z}_2 \\ &= -C_1 \cdot \|z_1\|^2 + z_1^T \cdot z_2 + z_2^T \cdot \{\dot{f}_{11}(x_1) \cdot x_2 - \ddot{q}_{ref}(t) \\ &\quad - \dot{a}_1(t) + f_{11}(x_1) \cdot g^* \cdot u + f_{11}(x_1) \cdot (W \cdot \phi + \varepsilon)\}\end{aligned}$$

Control Law is defined as follows.

$$\begin{aligned}u &= \{f_{11}(x_1) \cdot g^*\}^{-1} \cdot [\ddot{q}_{ref}(t) + \dot{a}_1(t) - z_1 - C_2 \cdot z_2 \\ &\quad - \dot{f}_{11}(x_1) \cdot x_2 - f_{11}(x_1) \cdot \hat{W} \cdot \phi]\end{aligned}\quad (7)$$

Letting $\tilde{W} = W^* - \hat{W}$, if $\hat{W} \cdot \phi$ approximates Δ , then $(\tilde{W} \cdot \phi + \varepsilon) \rightarrow 0$. Because $z_1^T \cdot z_2 = z_1 \cdot z_2^T$ exists, we obtain

$$\begin{aligned}\dot{V}_2 &= -C_1 \cdot \|z_1\|^2 - C_2 \cdot \|z_2\|^2 \\ &\quad + z_2^T \cdot f_{11}(x_1) \cdot (\tilde{W} \cdot \phi + \varepsilon) < 0\end{aligned}$$

and $z_2 \rightarrow 0$

B. Learning Algorithm of the Neural Network Controller

In order to obtain the adaptive law of the neural network weight, the third positive definite Lyapunov function V_3 is constructed as follows.

$$V_3 = V_2 + \frac{1}{2\gamma} \text{tr}(\tilde{W} \Gamma \tilde{W}^T) > 0$$

where Γ is a positive definite matrix, γ is a positive real number. Because $\text{tr}[z_2^T \cdot f_{11}(x_1) \cdot \tilde{W} \cdot \phi] = \text{tr}[\tilde{W} \cdot \phi \cdot z_2^T \cdot f_{11}(x_1)]$, then

$$\begin{aligned}\dot{V}_3 &= \dot{V}_2 + \frac{1}{\gamma} \text{tr}(\tilde{W} \Gamma \dot{\tilde{W}}^T) \\ &= -C_1 \cdot \|z_1\|^2 - C_2 \cdot \|z_2\|^2 + z_2^T \cdot f_{11}(x_1) \cdot (\tilde{W} \cdot \phi \\ &\quad + \varepsilon) + \frac{1}{\gamma} \text{tr}(\tilde{W}^T \Gamma \dot{\tilde{W}}^T) \\ &= -C_1 \cdot \|z_1\|^2 - C_2 \cdot \|z_2\|^2 + z_2^T \cdot f_{11}(x_1) \cdot \varepsilon \\ &\quad + \text{tr}[\tilde{W} \cdot (\phi \cdot z_2^T \cdot f_{11}(x_1) + \frac{1}{\gamma} \dot{\tilde{W}}^T)]\end{aligned}$$

If the adaptive learning algorithm of \hat{W} is designed as follows.

$$\dot{\hat{W}} = -\gamma \cdot \Gamma^{-1} \cdot \phi \cdot z_2^T \cdot f_{11}(x_1) - \gamma \cdot n \cdot \Gamma^{-1} \cdot \|z_2\| \cdot \hat{W} \quad (8)$$

then,

$$\begin{aligned}\dot{V}_3 &= -C_1 \cdot \|z_1\|^2 - C_2 \cdot \|z_2\|^2 + z_2^T \cdot f_{11}(x_1) \cdot \varepsilon \\ &\quad + \text{tr}(\tilde{W} \cdot n \cdot \|z_2\| \cdot \hat{W}) \\ &\leq -C_1 \cdot \|z_1\|^2 - C_2 \cdot \|z_2\|^2 + z_2^T \cdot f_{11}(x_1) \cdot \varepsilon \\ &\quad + n \cdot \|z_2\| \cdot (\|\tilde{W}\|_F \cdot \|W^*\|_F - \|\tilde{W}\|_F^2) \\ &\leq -C_1 \cdot \|z_1\|^2 - C_2 \cdot \|z_2\|^2 + z_2^T \cdot f_{11}(x_1) \cdot \varepsilon \\ &\quad + n \cdot \|z_2\| \cdot (\|\tilde{W}\|_F \cdot \varrho - \|\tilde{W}\|_F^2) \\ &= -C_1 \cdot \|z_1\|^2 - C_2 \cdot \|z_2\|^2 + z_2^T \cdot f_{11}(x_1) \cdot \varepsilon \\ &\quad - n \cdot \|z_2\| \cdot [(\|\tilde{W}\|_F - \frac{1}{2} \cdot \varrho)^2 - \frac{1}{4} \cdot \varrho^2]\end{aligned}$$

If $\|z_2\| \geq \frac{n \cdot \varrho^2 + 4 \|f_{11}(x_1)\| \cdot \|\varepsilon\|}{4C_2}$, then, $\dot{V}_3 < 0$.

Based on (7), (8), $n, C_1, C_2, \gamma, \Gamma$ are adjusted appropriately in order to make augmented state $z_1 \rightarrow 0, z_2 \rightarrow 0$ in the compact set $\Omega = \{z_2 \geq \frac{n \cdot \varrho^2 + 4 \|f_{11}(x_1)\| \cdot \|\varepsilon\|}{4C_2}\}$. Since $\varepsilon, \frac{n \cdot \varrho^2}{4C_2}$ can be adjusted to approximate arbitrarily small, Ω is considered to be a unrestricted set in a sense. That is, $x_1 \rightarrow q_{ref}(t)$, thus, tracing precision is guaranteed.

C. Control Law Allocation

Since outputs of control law (7) are moments along three axes and inputs of UAV are $\delta_e, \delta_a, \delta_r, \delta_x, \delta_y, \delta_z$, it's necessary to establish the mapping between moments and multiple control surfaces. In this section, pseudoinverse method is applied to realize the function of control law allocation. Equation (3) is expressed as follows.

$$\begin{bmatrix} L \\ M \\ N \end{bmatrix} = F + G \begin{bmatrix} \delta_e \\ \delta_a \\ \delta_r \\ \delta_x \\ \delta_y \\ \delta_z \end{bmatrix}$$

where

$$\begin{aligned}G &= \begin{bmatrix} 0 & \frac{1}{21.5} \delta C_{l\delta_a} Q \cdot S \cdot b & \frac{1}{30} \delta C_{l\delta_r} Q \cdot S \cdot b \\ 0 & 0 & 0 \\ 0 & \frac{1}{21.5} Q \cdot S \cdot b [\delta C_{n\delta_a} - \frac{1}{30} Q \cdot S \cdot b [\delta C_{n\delta_r} - \frac{1}{30} \delta C_{c\delta_a} (x_{cgr} - x_{cg}) \bar{b}] \\ \delta C_{c\delta_a} (x_{cgr} - x_{cg}) \bar{b}] & \delta C_{c\delta_r} (x_{cgr} - x_{cg}) \bar{b}] \\ -T \cdot y_T & -T \cdot z_T & 0 \\ 0 & 0 & T \cdot x_T \\ 0 & T \cdot x_T & 0 \end{bmatrix} \\ F &= \begin{bmatrix} \{C_{l_0} + \frac{b}{2V_T} (C_{l_r} r + C_{l_p} p)\} \\ T \cdot z_T + \{C_{m_0} + (C_{N_0} + \frac{q\bar{c}}{2V_T} C_{N_q}) (x_{cgr} - x_{cg}) \\ \{C_{n_0} + \frac{b}{2V_T} (C_{n_r} r + C_{n_p} p) + \delta C_{n\beta} \beta - (C_{c_0} + \delta C_{l\beta} \beta) \cdot Q \cdot S \cdot b \\ + \frac{q\bar{c}}{2V_T} C_{m_q}\} Q \cdot S \cdot \bar{c} \\ + \frac{rb}{2V_T} C_{c_r} + \frac{pb}{2V_T} C_{c_p}) (x_{cgr} - x_{cg}) \bar{b}\} Q \cdot S \cdot b \end{bmatrix}\end{aligned}$$

Letting

$$\Delta_{max} = \text{diag}(\delta_{e_{max}}, \delta_{a_{max}}, \delta_{r_{max}}, \delta_{x_{max}}, \delta_{y_{max}}, \delta_{z_{max}})$$

where $\delta_{i_{max}}, i = e, a, r, x, y, z$ denotes maximum deflection of corresponding control surface δ_i , therefore,

$$\begin{bmatrix} \delta_e \\ \delta_a \\ \delta_r \\ \delta_x \\ \delta_y \\ \delta_z \end{bmatrix} = \Delta_{max} (G \cdot \Delta_{max})^\dagger \left(\begin{bmatrix} L \\ M \\ N \end{bmatrix} - F \right) \quad (9)$$

where \dagger denotes pseudoinverse of certain matrix.

To sum up, the adaptive hybrid control scheme based on (7)~(9) can track attitude angles precisely.

IV. SIMULATION VALIDATION

To illustrate the validity of the hybrid control scheme, simulation of a UAV flight system is presented. The relevant parameters utilized in the simulations are listed as follows:

$$I_x = 12874.8 \text{ kg} \cdot \text{m}^2, I_y = 75673.6 \text{ kg} \cdot \text{m}^2$$

$$I_z = 85552.1 \text{ kg} \cdot \text{m}^2, I_{xz} = 1331.4 \text{ kg} \cdot \text{m}^2$$

Dynamic model of aileron, elevator, rudder actuator is: $\frac{20.2}{s+20.2}$. Magnitude and rate limits of aileron, elevator, rudder actuator are ± 25 degree, ± 60 degree/s respectively.

The UAV is trimmed at such a level flight condition, altitude: 6000 ft, velocity: 600 ft/s. Trim values are stated as follows.

$$T = 2535.7561 \text{ pound}$$

$$\delta_e = -1.7861 \text{ degree}$$

$$\delta_a = -5.6903 \cdot 10^{(-15)} \text{ degree}$$

$$\delta_r = -2.1258 \cdot 10^{(-14)} \text{ degree}$$

$$\alpha = 1.6505 \text{ degree}$$

Parameters of the control law are chosen as: $C_1 = 10.25, C_2 = 10.5$ and the node number of hidden layer in RBFNN is 40. In order to validate decouple and tracking performance of the scheme proposed, closed-loop flight system equipped with the hybrid controller is simulated. Given command of roll, pitch, yaw angle is all selected as $0.4 * \sin(t)$ (radian) signal, whose time responses are shown in Fig. 3 – Fig. 8. As can be seen from Fig. 3, given signals can be well tracked in the roll, pitch, yaw tunnels. Moment response of tracking given command is shown in Fig. 4. Fig. 5 – Fig. 6 show deflections of conventional control surface and thrust vector after allocation, which far exceed amplitude and rate constraints of the actuators. However, tracking performance of the closed-loop flight system also can be well guaranteed after allocation results pass through the actuators due to compensation of the neural network, which are shown in Fig. 7 – Fig. 8. Simulation results show that the UAV with the hybrid controller has good maneuverability, strong self-learning ability of compensating the unmodeled dynamics and enough robust stability against constraints of actuators.

V. CONCLUSION

A new hybrid control design scheme is proposed in this paper. From the discussion and simulation results, the following conclusions can be reached.

1. Linearization and decoupling of flight states are realized by employing backstepping method, which ensures the stability of nominal UAV dynamics throughout the flight envelope via twice “step back”.

2. A RBFNN compensator is adopted to ensure robust stability and performance of flight system, which is realized via the appropriate adaptive weighting matrix adjusting.

In such a design, there is no need to know the full information of UAV dynamics, therefore, the hybrid control design scheme is of practical use. However, how to eliminate

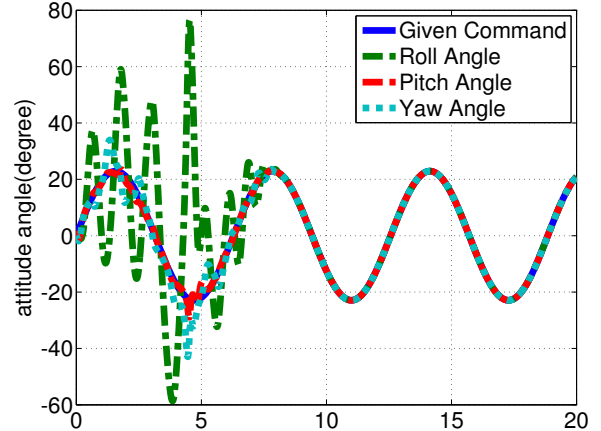


Fig. 3. Attitude angle time response of tracking $0.4 * \sin(t)$ (radian)

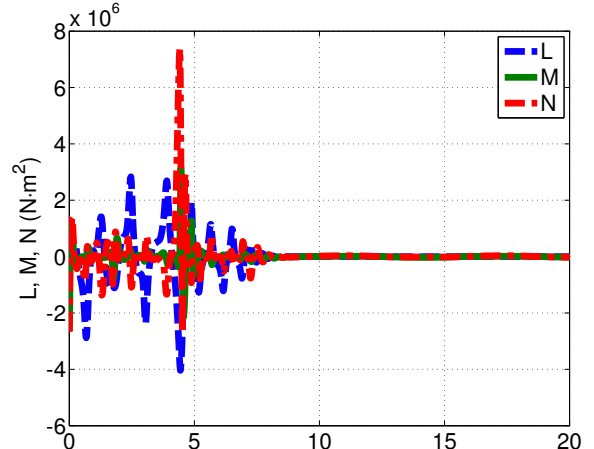


Fig. 4. Moment response of tracking $1.4 * \sin(t)$ (radian)

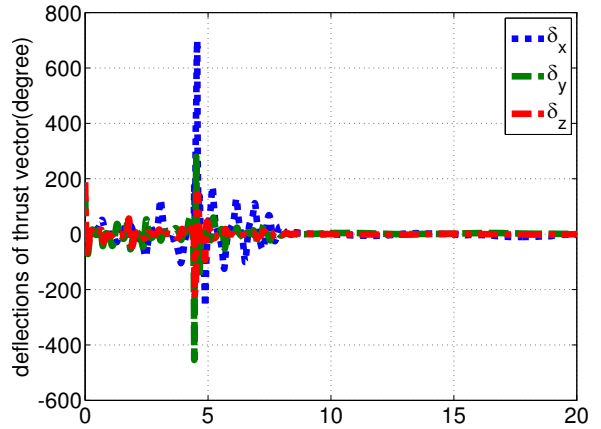


Fig. 5. Deflections of thrust vector after allocation

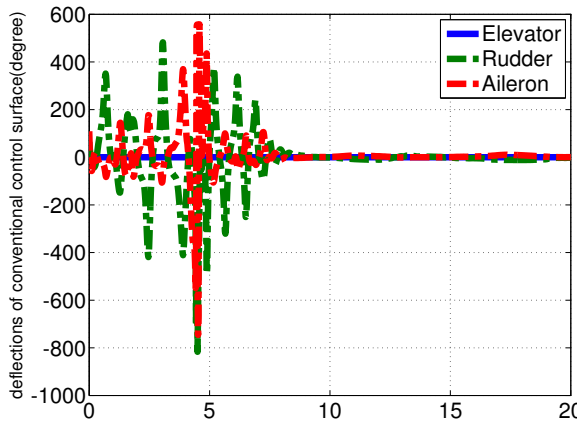


Fig. 6. Deflections of conventional control surface after allocation

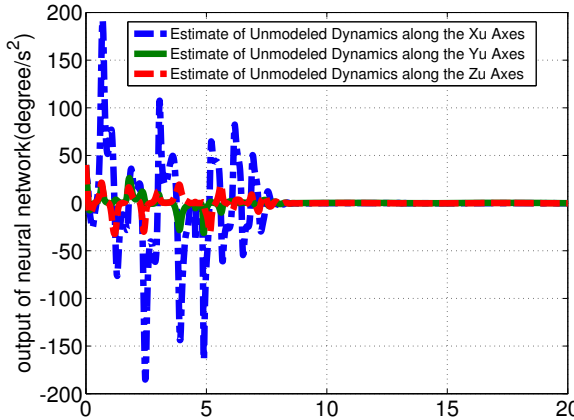


Fig. 7. Output of neural network for estimating unmodeled dynamics

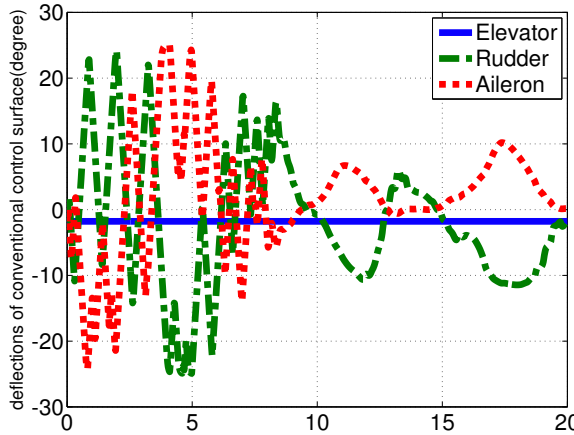


Fig. 8. Deflections of conventional control surface after allocation results pass through actuator

the adverse effect due to the constraint of control surfaces will be studied in further work.

VI. ACKNOWLEDGMENT

The author would like to thanks Dr. Ruyi Yuan for his useful discussion and help. The author also gratefully acknowledge reviewers' comments.

REFERENCES

- [1] Z. Xiong , and X. Dong, "Study and Outlook of Gain Scheduling Flight Control Law," *Flight Dynamics*, vol. 21, no. 4, pp. 9-13, December 2003
- [2] G. Cai, A. K. Cai, B. M. Chen and T. H. Lee, "Construction, Modeling and Control of a Mini Autonomous UAV Helicopter," *Proceedings of the IEEE International Conference on Automation and Logistics*, Qingdao, China, September 2008
- [3] Y. Fan, J. Zhu, C. Yang and Z. Sun, "Eigenstructure Assignment based Flight Control for Advanced Fighter : an Optimization based Approach," *The Third International Conference on Natural Computation*, August 2007
- [4] M. Chen, C. Jiang, and R. Mei, "Design of the Robust Guidance Law for Air-Air Missiles based on Mixed Control," *Control Technology of Tactical Missile*, no. 2, pp. 35-38, 2004
- [5] S. A. Snell, D. F. Enns, and W. L. Garrard, "Nonlinear Inversion Flight Control for a Supermaneuverable Aircraft," *Journal of Guidance, Control, and Dynamics*, vol. 15, no. 4, pp. 976-984, July-August 1992
- [6] T. Lee, Y. Kim, "Nonlinear Adaptive Flight Control Using Backstepping and Neural Networks Controller," *Journal of Guidance, Control, and Dynamics*, vol. 24, no. 4, pp. 675-682, July-August 2001
- [7] M. Sharma, and D. G. Ward, "Flight-Path Angle Control via Neuro-Adaptive Backstepping," *AIAA Guidance, Navigation and Control Conference and Exhibit*, 5-8 August 2002, Monterey, California
- [8] S. Liu, T. Zhu, and W. Yu, "Backstepping Theory and It's Application in the Nonlinear Flight Control System," *Journal of Aircraft Design*, vol. 27, no. 4, pp. 48-52, August 2007
- [9] A. D. Ngo, W. C. Reigelsperger, and S. S. Banda, "Tailless Aircraft Control Law Design Using Dynamic Inversion and Synthesis," *Proceedings of the 1996 IEEE International Conference On Control Applications*, Dearborn, MI , September 1996
- [10] E. N. Johnson, A. J. Calise, and J. E. Corban, "Adaptive Guidance and Control for Autonomous Launch Vehicles," *Aerospace Conference*, 2669-2682, March 2001, MT, USA
- [11] L. Sonneveldt, Q. P. Chu, and J. A. Mulder, "Nonlinear Flight Control Design Using Constrained Adaptive Backstepping," *Journal of Guidance, Control, and Dynamics*, vol. 30, no. 2, pp. 322-336, March-April 2007
- [12] L. Sonneveldt, Q. P. Chu, and J. A. Mulder, "Constrained Adaptive Backstepping Flight Control, Application to a Nonlinear F-16 MATV Model," *AIAA Guidance, Navigation and Control Conference and Exhibit*, 21-24 August 2006, Keystone, Colorado
- [13] M. Hagström, *Nonlinear Analysis and Synthesis Techniques in Aircraft Control*, Springer-Verlag Berlin Heidelberg, 2007
- [14] B. L. Stevens, F. L. Lewis, *Aircraft Control and Simulation(2nd Edition)*, John Wiley & Sons; 2003